

The effect of stiff substrates on the collective migration of A549 cells

SASAKI, Saori

Department of Mechanical Engineering, Faculty of Engineering, Kyushu University

DU, Zhaoyi

Department of Mechanical Engineering, Graduate school of Engineering, Kyushu University

TAKAHASHI, Ryu

Department of Mechanical Engineering, Graduate school of Engineering, Kyushu University

SUN, Qi

Department of Mechanical Engineering, Graduate school of Engineering, Kyushu University

他

<https://hdl.handle.net/2324/7167120>

出版情報 : Journal of Biomechanical Science and Engineering. 18 (4), pp.23-00298, 2023-12-25.

日本機械学会

バージョン :

権利関係 : © 2023 by The Japan Society of Mechanical Engineers



The effect of stiff substrates on the collective migration of A549 cells

Saori SASAKI*, Zhaoyi DU**, Ryu TAKAHASHI**, Qi SUN**, Toshihiro SERA***
and Susumu KUDO*

*Department of Mechanical Engineering, Faculty of Engineering, Kyushu University
744 Motooka Nishi-ku Fukuoka 819-0395, Japan
E-mail: kudo.susumu.237@m.kyushu-u.ac.jp

**Department of Mechanical Engineering, Graduate school of Engineering, Kyushu University
744 Motooka Nishi-ku Fukuoka 819-0395, Japan

*** Department of Medical and Robotic Engineering Design, Faculty of Advanced Engineering, Tokyo University of Science
6-3-1 Nijjuku Katsushika-ku Tokyo 125-8585, Japan

Received: 26 July 2023; Revised: 11 September 2023; Accepted: 15 September 2023

Abstract

The Young's modulus of normal lung tissues ranges from 1 to 5 kPa, whereas fibrotic or lung tumor tissues can be ~30 times stiffer. However, the lung parenchyma microscopically consists of various tissues, and cancer cells in tumors contact stiff collagen-containing fibers during invasion. In this study, we investigated the effect of stiff substrates on A549 cell migration. We fabricated stiff polydimethylsiloxane (PDMS) substrates with different stiffness levels (1.4, 3.4, and 18.3 MPa) by adjusting the cross-linking agent ratio. We examined the distance and the trajectory orientation of A549 cell migration on PDMS substrates and much stiffer 7.7 GPa glass with scratch-wound assays. A549 cells exhibited a collective sheet-like migration pattern toward the wounded area on stiff substrates. The migration range at 18.3 MPa was significantly higher than at 1.4 and 3.4 MPa, and that on glass was significantly higher than that at 18.3 MPa. The cell trajectory orientation on stiff PDMS substrates gradually increased and became constant, whereas that on glass was constant from the initial migration. Our results revealed that stiff substrates affect A549 cells migration in this range.

Keywords: Migration range, Effective distance, Cell trajectory orientation, Wound healing

1. Introduction

Cells sense extracellular environments to enable activities such as adhesion, proliferation, migration, apoptosis, and differentiation. Directional cell migration is critical for developmental morphogenesis and tissue homeostasis as well as disease progression in cancer. During migration, cells sense substrate stiffness through plasma-membrane receptors and move along stiffness gradients, a phenomenon known as “durotaxis” (Plotnikov et al., 2012).

For native soft tissues and organs, Young's modulus ranges from 0.1 kPa to 1 MPa, depending on the function and location of the tissue (Arda et al., 2011; Liu et al., 2015). In particular, Young's modulus of normal lung tissue ranges from 1 kPa to 5 kPa, and fibrotic/lung tumor tissue can be ~30 times stiffer (up to 150 kPa) (Shukla et al., 2016). Therefore, polydimethylsiloxane (PDMS) substrates used in durotaxis studies generally capture this stiffness range. Within this range of Young's modulus, increased matrix stiffness enhances the migration speed of individual isolated multiple glioma cells (Ulrich et al., 2009) and the collective migration speed of human mammary epithelial cells (Sunyer et al., 2016). Conversely, the opposite result was reported for single isolated rat kidney cells on a substrate of similar stiffness (Pelham and Wang, 1997). Moreover, on stiffer substrates (1.5 MPa, 4.8 MPa, and tissue culture polystyrene dishes), A549 human lung cancer cells showed a statistically significant decrease in the accumulated distance and average speed with increasing substrate stiffness (Shukla et al., 2016). These opposite results suggest that cell migration is biphasic concerning substrate stiffness. Migration speed may rise and then fall, exhibiting a maximal migration at an intermediate stiffness depending on the cell type (Bangasser et al., 2013, 2017).

A previous study reported that A549 cells were “stiffness-dependent,” and their migration speed was higher on a 4.8 kPa substrate than on a 150 Pa substrate (Tilghman et al., 2010). On the other hand, the migration distance and speed of A549 cells gradually decreased on substrates with Young’s modulus ranging from 27 kPa to 4.8 MPa and a polystyrene dish (Shukla et al., 2016). Although Young’s modulus of normal lung tissue was measured using atomic force microscopy and was less than 5 kPa (Liu and Tschumperlin, 2011), lung parenchyma consists of various tissues, such as elastin, collagen, and smooth muscle cells. In particular, Young’s moduli of elastin and collagen are 0.3–1.0 and 100–1000 MPa, respectively (Camasão and Mantovani, 2021). During tumor invasion, cancer cells contact collagen-containing fibers (Condeelis and Segall, 2003; Wang et al., 2002).

Until now, most of our understanding of the cell migration is obtained from the studies using single isolated cells. However, fundamental processes during some forms of cancer cell invasion are driven by migration of cell groups. Intercellular interactions within cell groups may influence the mechanism of cancer cell migration (Sunyer et al., 2016). Additionally, various parameters, such as migration distance, area, speed, and trajectory orientation, are used to evaluate the migration behavior. In particular, the trajectory orientation assesses the directed cell migration in a preferred direction, and the orientation is higher on polystyrene dishes than PDMS substrates ranging from 27 kPa to 4.8 MPa (Shukla et al., 2016). In this study, we focused on stiffer substrates (ranging from 1 MPa to 20 MPa) than lung parenchyma and investigated the effect of stiff substrates on the collective migration of A549 cells. For this purpose, we fabricated PDMS substrates with different stiffness levels by adjusting the cross-linking agent ratio and examined changes in the individual cell migration, such as the migration distance and cell trajectory orientation, with scratch-wound assays.

2. Method

2.1 Preparation of substrate

We used SYLGARD184 polydimethylsiloxane elastomer (Dow Corning, Midland, MI, USA), which consists of a prepolymer and crosslinker. PDMS stiffness can be adjusted by adding different amounts of the crosslinker into the prepolymer solution and baking for a certain amount of time. In this study, the prepolymer was mixed with 5%, 10%, and 20% crosslinker to obtain three types of samples. Then, these mixed liquids were degassed with a vacuum pump for 1 h, dropped in 1-ml aliquots into a glass dish, and heated at 60°C for 3 h to solidify the PDMS substrate on the bottom of the glass dish. For comparison, a 7.7-GPa glass base dish (Matsunami, Osaka, Japan) was prepared as a much stiffer substrate.

We assessed Young’s modulus of PDMS with different concentrations of the crosslinker. The surface images of the swollen gels were obtained using an atomic force microscope (AFM) system (Dimension Icon AFM, Bruker). The probe was silicon nitride (SNL-10A, Bruker), and the measurement mode was peak force tapping mode. The stiffness of PDMS was estimated by the indentation test within a $25 \times 25 \mu\text{m}^2$ area.

2.2 Cell culture

In this study, A549 lung cancer cells (JCRB0076, provided by the Japanese Cancer Research Resources Bank, Japan) were cultured in Dulbecco’s modified eagle medium (DMEM; Gibco, Thermo Fisher Scientific, Waltham, MA, USA) containing 10% fetal bovine serum (FBS, Gibco, Thermo Fisher Scientific), and a 1% antibiotic-antifungal agent (10,000 U/ml penicillin, 10,000 mg/ml streptomycin, and 25 mg/ml amphotericin) (Gibco, Thermo Fisher Scientific). A549 cells were grown to confluence in 50 $\mu\text{g}/\text{ml}$ fibronectine (Sigma-Aldrich, St. Louis, MO, USA)-coated PDMS and glass dishes.

2.3 Scratch-wound assay

A scratch-wound was produced in cell monolayers using CELL Scratcher (IWAKI Glass, Chiba, Japan). Traditionally, wounded scratch is performed by pipet tips (Liang et al., 2007; Sera et al., 2018), but there is a risk of the disruption of the surface of the substrate (Ashby et al., 2012). In contrast, the tip of this scratch in this study was made of silicon preventing the damage to the substrate. Immediately after scratching, the medium was exchanged from DMEM to L-15(+) medium, which was prepared by adding 10% FBS and 1% antibiotics to Leibovitz’s L-15 Medium (Gibco, Thermo Fisher Scientific). Cell migration was observed with an inverted fluorescence microscope (ECLIPSE Ti2E, Nikon, Tokyo, Japan) and a 10 \times objective lens (Nikon S Fluor 10x, Nikon) for 12 h. The temperature was maintained at 35.5°C–37.5°C. Time-lapse images were captured each hour using a camera (DS-Qi2, Nikon) controlled by imaging software (NIS-Elements, Nikon).

2.4 Image analysis

We performed three independent experiments, and randomly chose 60 cells from the frontier cells facing the scratched area for each substrate and traced their migration paths ($N = 3$, $n = 180$). The manual tracking tool, an ImageJ software (NIH) plugin, was used to analyze cell migration. To determine the origin of the cell automatically, the shape of the individual cell should be analyzed first. However, it is difficult to determine the shape because the boundary is not clear. Moreover, during cell migration, membrane protrusions like the lamellipodium and filopodium are formed, which may influence the origin of the cell. Therefore, the positions of individual cells were determined visually based on the center of the cell. Three parameters were employed to quantify the migration behavior of the cells: migration range, effective distance, and cell trajectory orientation (Tanaka et al., 2005). These parameters were calculated using the coordinates of each cell, which was captured by manual tracking. Migration range and effective distance were defined as follows,

$$\text{Migration range} = \sum_{i=1}^m \sqrt{(x_i - x_{i-1})^2 + (y_i - y_{i-1})^2} \quad (1)$$

$$\text{Effective distance} = \sum_{i=1}^m (y_i - y_{i-1}) \quad (2)$$

where m is the number of acquisitions, and x_i and y_i are the distance of each axis from the origin (time = 0) at i times acquisition, when the direction of the wounded area is defined as the y -axis (Fig. 1). Cell trajectory orientation was defined as the angle between the net increment of the cell in the x -direction and the net increment of the cell in the y -direction. A cell trajectory orientation value of 90° means that A549 cells migrate along the y -axis. Additionally, the average migration speed was calculated based on migration range for each cell over the course of each experiment.

2.5 Statistical analysis

Statistical analysis was performed with analysis of variance; multiple comparisons were performed using Tukey's test. A difference indicates that there is a significant difference at $p < 0.05$.

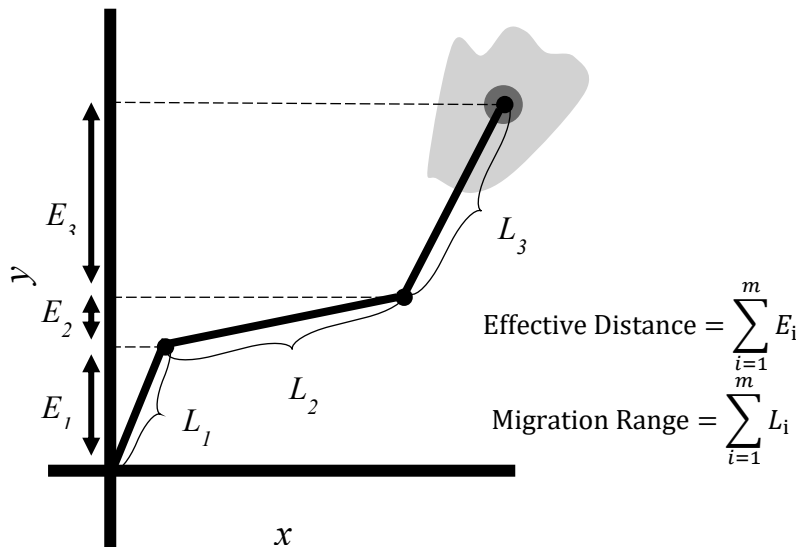


Fig. 1 Calculation of the effective distance and migration range of A549 cells.

3. Results and discussion

In this study, AFM was used to measure Young's modulus of PDMS with different concentrations of the crosslinker. Young's modulus values were estimated to be 1.4 ± 0.5 (average \pm S.D.) MPa (5%), 3.4 ± 3.3 MPa (10%), and 18.3 ± 6.4 MPa (20%).

Figure 2 shows representative images of A549 cell migration on (A) 1.4 MPa, (B) 3.4 MPa, (C) 18.3 MPa, and (D) 7.7GPa substrates. The cells exhibited a collective sheet-like migration pattern toward the wounded area, consistent with

a previous study investigating the cell migration of soft substrate and stiff tissue culture polystyrene (Ashby et al., 2012; Ng et al., 2012; Shukla et al., 2016). The cells on a soft substrate of 27 kPa quickly became isolated with fewer cell-cell contacts and exhibited a more random individual cell migration pattern (Shukla et al., 2016). Figure 3 shows a representative trajectory of cell migration, and the starting position of each trajectory was set as the origin ($N = 3$, $n = 50$). In this study, the wound edge was irregular because it was difficult to scrape the cells straight. Therefore, the cells could migrate horizontally at initial stage. Figure 4A shows the migration range after the wound scratch. At 12 h, the migration ranges were $92.6 \pm 18.3 \mu\text{m}$ (average \pm S.D.) at 1.4 MPa, $85.7 \pm 18.8 \mu\text{m}$ at 3.4 MPa, and $120.1 \pm 26.2 \mu\text{m}$ at

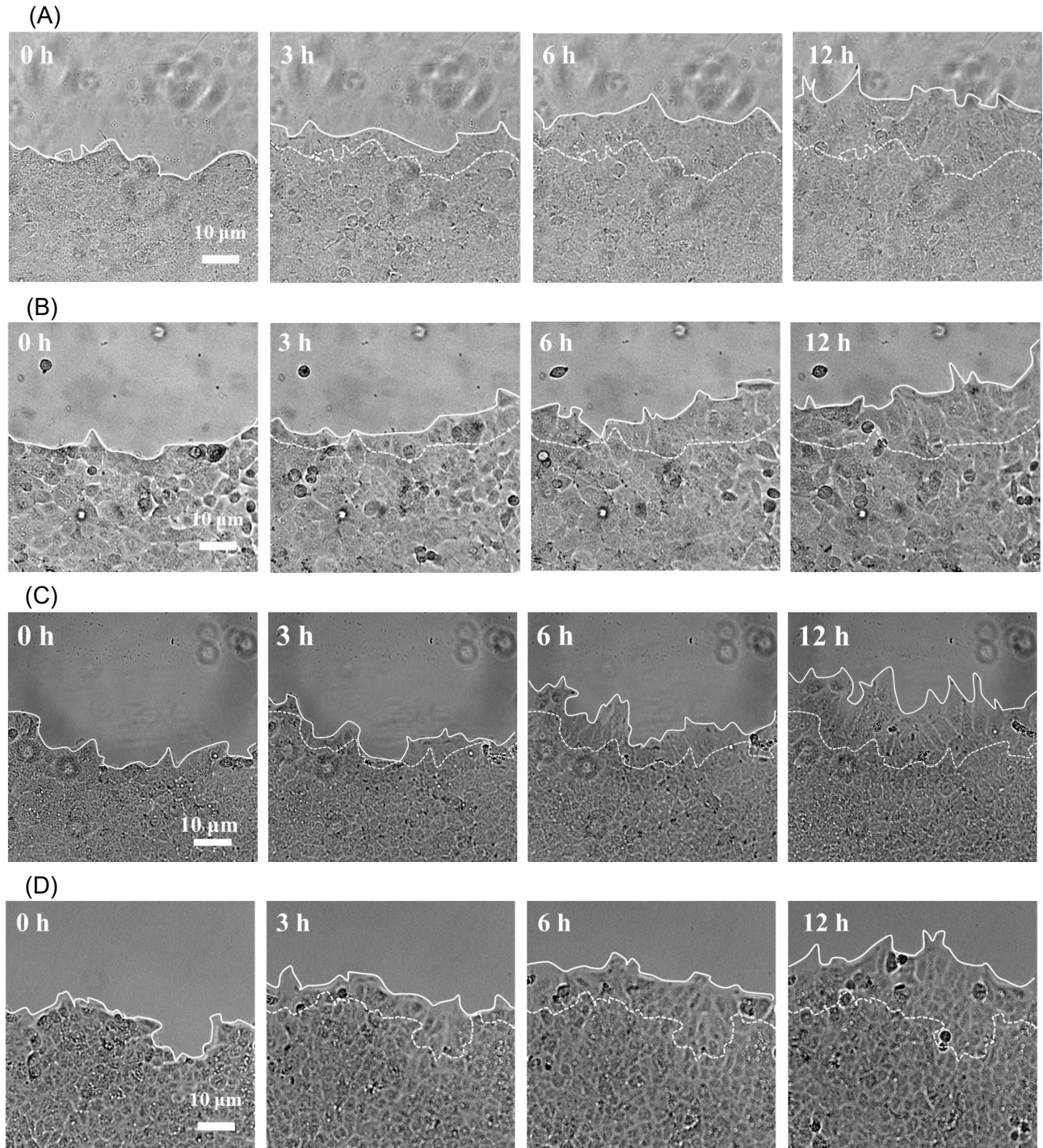


Fig. 2 Representative microscopic images of A549 cells migrating to the wounded area on (A) 1.4 MPa, (B) 3.4 MPa, (C) 18.3 MPa, and (D) 7.7 GPa substrates. The solid and dotted lines show the edges of the cell migration at each time and 0 h, respectively. The scale bar is 10 μm .

18.3 MPa. The migration range at 18.3 MPa was significantly higher than that at 1.4 and 3.4 MPa after 2 h. Compared to 3.4 MPa, the migration range at 1.4 MPa was significantly higher at 11 and 12 h. The migration range on 7.7 GPa glass was $126.1 \pm 27.5 \mu\text{m}$ after 12 h. Furthermore, it was significantly higher than 18.3 MPa after 2 h. In the tested stiffness range, an increase in matrix stiffness promoted the collective migration of A549 cells, and the average migration speed was 7.7, 7.1, and $10.0 \mu\text{m/hr}$ at 1.4, 3.4, and 18.3 MPa, respectively. Conversely, previous studies of A549 cells mainly focused on the cell migration on softer substrates. A previous study reported that the speed was 10 and $25 \mu\text{m/hr}$ at 0.15 and 4.8 kPa, respectively, and that cells on a 4.8-kPa substrate exhibited prominent stress fibers and focal adhesions and decreased E-cadherin expression (Tilghman et al., 2010). Another study reported that the speed as 9 and $11 \mu\text{m/hr}$ at 1 and 11 kPa, respectively (Ashby et al., 2012). Moreover, the speed was approximately 39 and $30 \mu\text{m/hr}$ at 27 and 4756 kPa, respectively, and increased substrate stiffness led to slower migration (Shukla et al., 2016). Particularly, at 27 kPa soft substrate, cells quickly become isolated and exhibit a more random individual migration pattern, and the phosphorylated focal adhesion kinase and paxillin levels decreased on stiff substrates, which correlated with slow migration. Furthermore, the speed on tissue culture polystyrene was $\sim 18 \mu\text{m/hr}$ (Shukla et al., 2016), whereas that on 7.7 GPa glass was $10.5 \mu\text{m/hr}$ in this study. These results suggest that A549 cell migration is biphasic with respect to substrate stiffness as a theoretical motor-clutch model in a previous study (Bangasser et al., 2013). In this model, the self-assembly of F-actin at the plasma membrane pushes the membrane forward, on the other hand myosin motors pull F-actin rearward

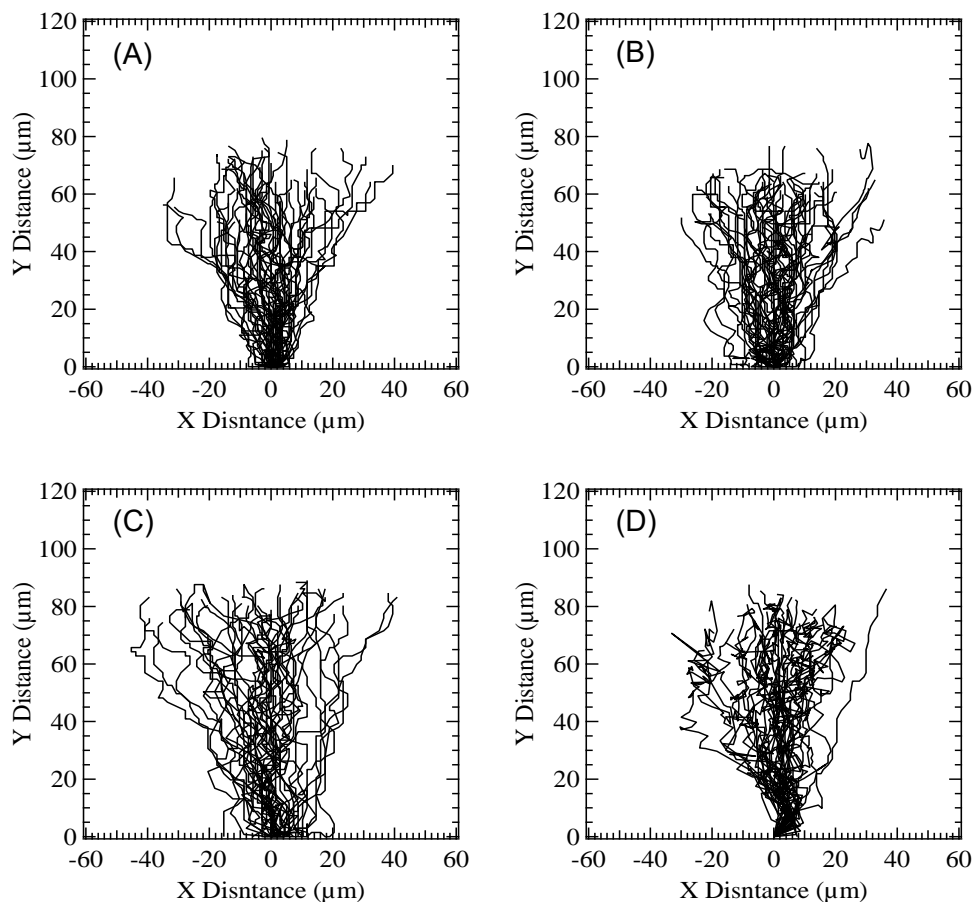


Fig. 3 Representative migration trajectories of each cell on (A) 1.4 MPa, (B) 3.4 MPa, (C) 18.3 MPa, and (D) 7.7GPa substrates ($N=3$, $n = 50$).

to induce the retrograde flow of F-actin. Intracellular molecular “motors”, such as myosin II, transmit force to the external environment through rigid actin filament bundles and compliant transmembrane molecular “clutches”, such as integrin (Mitchison and Kirschner, 1988; Bangasser et al., 2013, 2017). According to this model, clutches quickly build force and fail on a stiff substrate, whereas clutches fail spontaneously before motors load the substrate appreciably on a soft substrate, and the maximum traction force exists between the two states (Bangasser et al., 2013).

On the other hand, the speed was $7.1 \mu\text{m/h}$ at 3.4 MPa in this study, whereas it was approximately $30 \mu\text{m/h}$ at 4756 kPa (Shukla et al., 2016). The speed in this study tends to be slower than that reported in previous study. In both studies,

the cells were cultured to form a confluent monolayer before scratch assay. However, the cell-cell contact seems to be insufficient after scratch in previous study, resulting that the cells migrate more randomly and the speed may be higher than our result. On softer substrate (0.15 and 4.8 kPa) in previous study (Tilghman et al., 2010) the migration was evaluated for individual isolated cell, and migration speed is higher for isolated cell than that clustered cell (Lalli and Asthagiri et al., 2015). Furthermore, our results did not show the biphasic migration. The speed of collective migration on soft substrates (1 and 10 kPa) was 9 and 11 $\mu\text{m}/\text{h}$, respectively (Ashby et al., 2012), indicating that the Young's modulus of the substrate for maximal speed may be ranged from 10 kPa to 3.4 MPa. Indeed, in spite of depending on cell type, the optimal Young's modulus was estimated at approximately 100 kPa for different cancer cell, U87 glioma cells (Bangasser et al., 2013)

To investigate the migration patterns, we calculated the effective distance as the y-axis component of cell migration and the cell trajectory orientation as the effective direction of migration (Fig. 4B and 4C). Particularly, the cells migrated toward the wounded area macroscopically, however the trajectory was random microscopically (Fig. 3). Therefore, the orientation at each time was evaluate from the origin. The effective distance after 12 h was $70.0 \pm 19.2 \mu\text{m}$ at 1.4 MPa, $61.9 \pm 15.2 \mu\text{m}$ at 3.4 MPa, and $79.0 \pm 19.6 \mu\text{m}$ at 18.3 MPa. It was significantly higher at 18.3 MPa than at 1.4 and 3.4 MPa after 5 h. Compared to 3.4 MPa, the effective distance at 1.4 MPa was significantly higher after 2 h. Regarding the cell trajectory orientation, in the initial hour, it was $55.7.2 \pm 28.5^\circ$ on 1.4 MPa, $40.2 \pm 33.7^\circ$ on 3.4 MPa, and $36.5 \pm 43.8^\circ$ on 18.3 MPa. The cell trajectory orientation on all substrates gradually increased during migration, and there was no significant difference between the substrate stiffness after 5 h. The orientation angle was $\sim 75^\circ$. These results show that individual A549 cells on stiff substrate in this range gradually migrate directly toward the wounded area during collective sheet-like migration. In particular, the cell trajectory orientation at 18.3 MPa tended to be lower than that at 1.4 and 3.4 MPa during the early migration stage. Indeed, the orientation at 18.3 MPa was significantly lower than that at 1.4 MPa after 1–4 h and was significantly lower than that at 3.4 MPa after 2 and 3 h. Although the effective distance was not significantly different from 1.4 and 3.4 MPa until 5 h, the migration range was higher. These results indicate that A549 cells migrate more randomly on 18.3 MPa during the early migration stage. Indeed, the migration trajectories seems to be random initially (Fig. 3C) and the S.D. of orientation is larger (Fig. 4C). After 12h, the migration range and the effective distance was significantly higher on 18.3 MPa than others even though the orientation angel was approximately same, suggesting that directional speed became higher than other substrates. Previous study reported that cell polarization is important for directional migration (Ridley et al., 2003), and in case of mammary epithelial cells (MCF10A), the wound edge cells on 65 kPa substrate were polarized with the Golgi anterior to the nucleus early in wound-healing process more than on 3 kPa substrate (Ng et al., 2012).

On 7.7 GPa glass, the effective distance was $72.7 \pm 18.1 \mu\text{m}$ after 12 h, and it tended to be higher than on other substrates, although it was lower than 18.3 MPa after 10 h. Particularly, in the initial hour, the effective distance was $16.2 \pm 6.3 \mu\text{m}$ and was significantly higher than on other substrates ($5.6 \pm 3.9 \mu\text{m}$ at 1.4 MPa, $3.4 \pm 2.9 \mu\text{m}$ at 3.4 MPa, and $5.2 \pm 6.9 \mu\text{m}$ at 18.3 MPa). The cell trajectory orientation was $68.7 \pm 18.4^\circ$ after 1 h, which was significantly larger than

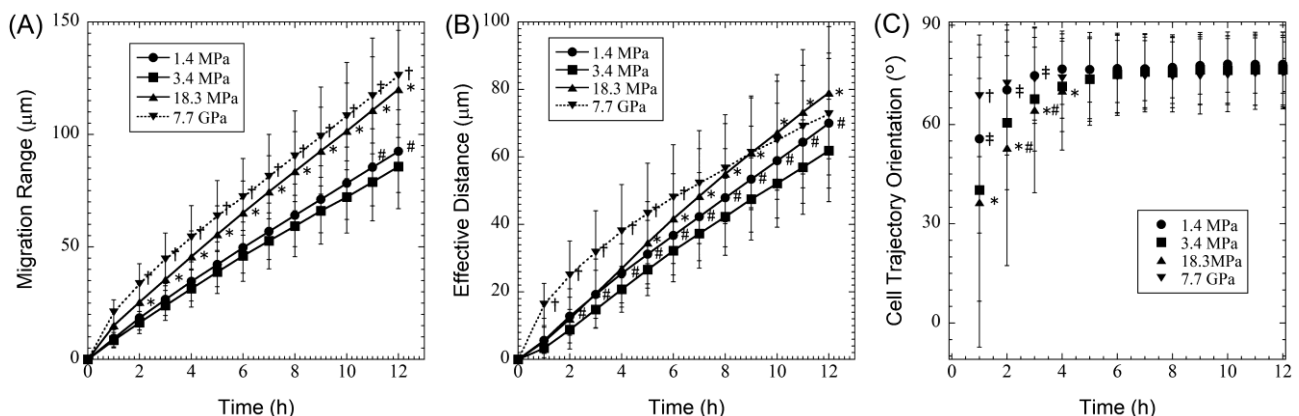


Fig. 4 A549 cell migration on substrates with different stiffness levels over 12 h (N = 3, n = 180). (A) Migration range. * $p < 0.05$ vs. substrates with 1.4 and 3.4 MPa, # $p < 0.05$ vs. substrate with 3.4 MPa, and † $p < 0.05$ vs. substrate with 18.3 MPa. (B) Effective distance. * $p < 0.05$ vs. substrates with 1.4 and 3.4 MPa, # $p < 0.05$ vs. substrate with 3.4 MPa, and † $p < 0.05$ vs. substrate with 18.3 MPa. (C) Trajectory orientation index. * $p < 0.05$ vs. substrate with 1.4 MP, # $p < 0.05$ vs. substrate with 3.4 MPa, and † $p < 0.05$ vs. substrate with 1.4, 3.4, and 18.3 MPa, ‡ $p < 0.05$ vs. substrate with 3.4 MPa.

on the other substrates. The orientation was $75.6 \pm 10.8^\circ$ after 12 h. A previous study reported that A549 cells on tissue culture polystyrene directionally migrate more after 24h (Shukla et al., 2016). Our results indicate that individual A549 cells on 7.7 GPa glass exhibit a direct migration during collective sheet-like migration from the outset.

In summary, cancer cells in tumors contact stiff collagen-containing fibers during invasion. Therefore, in this study, we prepared substrates with stiffness levels of 1.4, 3.4, and 18.3 MPa, stiffer than lung parenchyma, and investigated the effects of stiff substrate on A549 cell migration with wound scratch assays. The cells exhibited a collective sheet-like migration pattern toward the wounded area, and an increase in matrix stiffness promoted A549 cell migration, not biphasic behavior, in the tested stiffness range. On 18.4 MPa substrate, the cells migrated randomly during early stage and the speed was gradually higher than other substrates. On much stiffer 7.7 GPa glass, individual cells exhibit a direct migration from the outset. Our results revealed that stiff substrates tend to be enhanced the collective migration speed of A549 cells, however, on soft substrate, possibly between 10 kPa – 3.4 MPa, the migration speed may be faster due to the biphasic migration.

Acknowledgements

This research was partially supported by JSPS KAKENHI (Grant Number JP19H04444 and JP20K20183), Takahashi Industrial and Economic Research Foundation, and JKA and its promotion fund from AUTORACE.

References

- Arda, K., Ciledag, N., Aktas, E., Aribas, B.K., Köse, K., Quantitative assessment of normal soft-tissue elasticity using shear-wave ultrasound elastography, *American journal of roentgenology*, Vol. 197, (2011), pp.532–536.
- Ashby, W.J., Wikswo, J.P., Zijlstra, A., Magnetically attachable stencils and the non-destructive analysis of the contribution made by the underlying matrix to cell migration, Vol. 33, (2012), pp.8189–8203.
- Bangasser, B.L., Rosenfeld, S.S., Odde, D.J., Determinants of Maximal Force Transmission in a Motor-Clutch Model of Cell Traction in a Compliant Microenvironment, *Biophysical Journal*, Vol. 105, (2013), pp.581–592.
- Bangasser, B.L., Shamsan, G.A., Chan, C.E., Opoku, K.N., Tüzel, E., Schlichtmann, B.W., Kasim, J.A., Fuller, B.J., McCollough, B.R., Rosenfeld, S.S., Odde, D.J., Shifting the optimal stiffness for cell migration, *Nature Communications*, Vol. 8, (2017), DOI: 10.1038/ncomms15313.
- Camasão, D.B., Mantovani, D., The mechanical characterization of blood vessels and their substitutes in the continuous quest for physiological-relevant performances. A critical review, *Materials Today Bio*, Vol. 10, (2021), DOI: 10.1016/j.mtbio.2021.100106.
- Condeelis, J., Segall, J.E., Intravital imaging of cell movement in tumours, *Nature Reviews. Cancer*, Vol. 3, (2003), pp.921–930.
- Lalli, M.L., Asthagiri, A.R., Collective migration exhibits greater sensitivity but slower dynamics of alignment to applied electric fields, *Cellular and molecular bioengineering*, Vol. 8, (2015), pp.247–257.
- Liang, C.C., Park, A.Y., Guan J.L., In vitro scratch assay: a convenient and inexpensive method for analysis of cell migration in vitro., *Nature Protocols*, Vol. 2, (2007), pp.329–333.
- Liu, F., Tschumperlin, D.J., Micro-Mechanical Characterization of Lung Tissue Using Atomic Force Microscopy, *Journal of Visualized Experiments*, Vol. 54, (2011), DOI: 10.3791/2911.
- Liu, J., Zheng, H., Poh, P.S.P., Machens, H.-G., Schilling, A.F., Hydrogels for Engineering of Perfusable Vascular Networks, *International Journal of Molecular Sciences*, Vol. 16, (2015), pp.15997–16016.
- Mitchison, T., Kirschner, M., Cytoskeletal dynamics and nerve growth, *Neuron*, Vol. 1, (1988), pp.761–772.
- Ng, M.R., Besser, A., Danuser, G., Brugge, J.S., Substrate stiffness regulates cadherin-dependent collective migration through myosin-II contractility, Vol. 199, (2012), pp.545–563.
- Pelham, R.J., Wang, Y. I, Cell locomotion and focal adhesions are regulated by substrate flexibility, *Proceedings of the National Academy of Sciences of the United States of America*, Vol. 94, (1997), pp.13661–13665.
- Plotnikov, S.V., Pasapera, A.M., Sabass, B., Waterman, C.M., Force Fluctuations within Focal Adhesions Mediate ECM-Rigidity Sensing to Guide Directed Cell Migration, *Cell*, Vol. 151, (2012), pp.1513–1527.
- Ridley, A.J., Schwartz, M.A., Burridge, K., Firtel, R.A., Ginsberg, M.H., Borsiy, G., Parsons, J.T., Horwitz, A.R., Cell migration: integrating signals from front to back, Vol. 302, (2003), pp.1704–1709.

- Shukla, V.C., Higueta-Castro, N., Nana-Sinkam, P., Ghadiali, S.N., Substrate stiffness modulates lung cancer cell migration but not epithelial to mesenchymal transition, *Journal of Biomedical Materials Research. Part A*, Vol. 104, (2016), pp.1182–1193.
- Sera, T., Sumii, T., Fujita, R., Kudo, S., Effect of shear stress on the migration of hepatic stellate cells, *In Vitro Cellular & Developmental Biology. Animal*, Vol. 54, (2018), pp.11–22.
- Sunyer, R., Conte, V., Escribano, J., Elosegui-Artola, A., Labernadie, A., Valon, L., Navajas, D., García-Aznar, J.M., Muñoz, J.J., Roca-Cusachs, P., Trepats, X., Collective cell durotaxis emerges from long-range intercellular force transmission, *Science*, Vol. 353, (2016), pp.1157–1161.
- Tanaka, T., Naruse, K., Sokabe, M., Effects of mechanical stresses on the migrating behavior of endothelial cells, *Biomechanics at Micro- and Nanoscale Levels.*, (2005), pp.75–87. WORLD SCIENTIFIC.
- Tilghman, R.W., Cowan, C.R., Mih, J.D., Koryakina, Y., Gioeli, D., Slack-Davis, J.K., Blackman, B.R., Tschumperlin, D.J., Parsons, J.T., Matrix rigidity regulates cancer cell growth and cellular phenotype, *PLoS One*, Vol. 5, (2010), DOI: 10.1371/journal.pone.0012905.
- Ulrich, T.A., de Juan Pardo, E.M., Kumar, S., The mechanical rigidity of the extracellular matrix regulates the structure, motility, and proliferation of glioma cells, *Cancer Research*, Vol. 69, (2009), pp.4167–4174.
- Wang, W., Wyckoff, J.B., Frohlich, V.C., Olynykov, Y., Hüttelmaier, S., Zavadil, J., Cermak, L., Bottinger, E.P., Singer, R.H., White, J.G., Segall, J.E., Condeelis, J.S., Single cell behavior in metastatic primary mammary tumors correlated with gene expression patterns revealed by molecular profiling, *Cancer Research*, Vol. 62, (2002), pp.6278–6288.